Thermochimica Acta 505 (2010) 69–72

Contents lists available at ScienceDirect

Thermochimica Acta

journal homepage: www.elsevier.com/locate/tca

Studies on the phase diagram of $CaCl_2$–$CaBr_2$ system

Sajal Ghosh, R. Sridharan, T. Gnanasekaran*

Liquid Metals and Structural Chemistry Division, Indira Gandhi Centre for Atomic Research, Kalpakkam 603102, India

ARTICLE INFO

Article history:
Received 17 November 2009
Received in revised form 25 March 2010
Accepted 31 March 2010
Available online 8 April 2010

Keywords:
Binary phase diagrams
CaCl2–CaBr2 system
Differential thermal analysis
X-ray characterization
Alkaline earth halides
Solid solution

ABSTRACT

A study on pseudo-binary $CaCl_2$–$CaBr_2$ system was carried out using differential thermal analysis (DTA) technique covering the complete composition range of the constituents between room temperature and 1073 K. From the DTA results the contour of solidus and liquidus temperatures with composition are plotted and the phase diagram of $CaCl_2$–$CaBr_2$ system is constructed. The solidus and liquidus curves exhibit a minimum at 971 K and at a composition of 56.5 mol% $CaBr_2$. Below 971 K, the system exhibits complete solid solution. Long-term equilibration of samples of several compositions was carried out at 923 and 673 K and the phases were characterized by XRD. The XRD results supported solid solution formation in the $CaCl_2$–$CaBr_2$ system between 673 and 923 K.

1. Introduction

Hydride ion conducting electrolytes are used in electrochemical sensors for detecting hydrogen in liquid sodium coolant of fast reactors [1,2]. In this regard, several combinations of alkali/alkaline earth halides mixed with alkali/alkaline earth hydrides such as LiCl–KCl containing 0.2–2 mol% LiH [2], $CaCl_2$–CaH_2 [3,4], a ternary mixture of LiCl, $CaCl_2$ and CaHCl [5] and binary CaHBr–$CaBr_2$ [6] systems have been investigated for using them as hydride ion conducting electrolytes. Physical properties viz. thermal conductivity and mechanical integrity of solid electrolyte systems containing the hydride ion conducting phases like CaHCl and CaHBr depend upon other phases present and the relevant phase diagrams. Binary phase diagrams of LiCl–$CaCl_2$ as well as that of LiBr–$SrBr_2$ systems were established by us earlier [7,8]. In this work, the binary phase diagram of $CaCl_2$–$CaBr_2$ system has been investigated by differential thermal analysis (DTA) and by identifying equilibrium phases that co-exist by X-ray diffraction (XRD) and the results are reported.

2. Experimental

Calcium bromide was prepared by reacting $CaCO_3$ (Sigma–Aldrich, chelometric standard, A.C.S. reagent) and distilled AR grade HBr (Merck, 47.8% azeotropic) solution. The resultant $CaBr_2$ solution was concentrated over a hot plate and dried under flowing argon gas. Dry $CaBr_2$ obtained thus was further purified by heating it up to its melting point in a quartz crucible placed in a quartz vessel in a stream of dry argon gas containing HBr for 2 h to remove any trace of volatile impurities. In a similar way $CaCl_2$ (99.9%, M/s. Alfa Products, USA) was further purified by heating it up to its melting point in a stream of dry argon gas carrying HCl for 2 h. The purified salts were then cooled to room temperature and transferred into a high purity argon atmosphere glove box that is used for handling liquid sodium. Calculated amounts of purified $CaCl_2$ and $CaBr_2$ were mixed to prepare samples of varying compositions. Weighing, mixing and pelletising of these samples were carried out in the argon atmosphere glove box. Before the DTA run, sample was brought out of the glove box and loaded into the DTA apparatus (SETSYS Evolution 16/18, M/s. Setaram, France). While loading the samples (~15 mg) in the DTA apparatus, the sample got exposed to air for a very brief time (~1 min.). In order to remove the moisture picked up during this process, the samples were first heated in the DTA apparatus under flowing argon gas at 573 K for 1 h. Removal of moisture was confirmed from the thermo gravimetric (TG) data and by measuring the melting points of the pure components. Argon gas was used at a flow rate of 20 ml/min during all the experiments. Because appreciable super-cooling effects were observed during cooling runs with this system, temperatures corresponding to various thermal events were obtained from the analysis of the DTA curves of heating runs only. DTA runs were recorded with a heating rate of 5 K/min from room temperature to 923 K and at a rate of 1 K/min from 923 to 1073 K. Several DTA runs were carried out with each sample so as to obtain concordant data (reproducible to within ±1 °C) while first run was

* Corresponding author at: Liquid Metals & Structural Chemistry Division, Chemistry Group, Indira Gandhi Center for Atomic Research, Kalpakkam 603102, India. Tel.: +91 44 27480302; fax: +91 44 27480065.
E-mail address: gnani@igcar.gov.in (T. Gnanasekaran).

0040-6031/$ – see front matter © 2010 Elsevier B.V. All rights reserved.
doi:10.1016/j.tca.2010.03.027

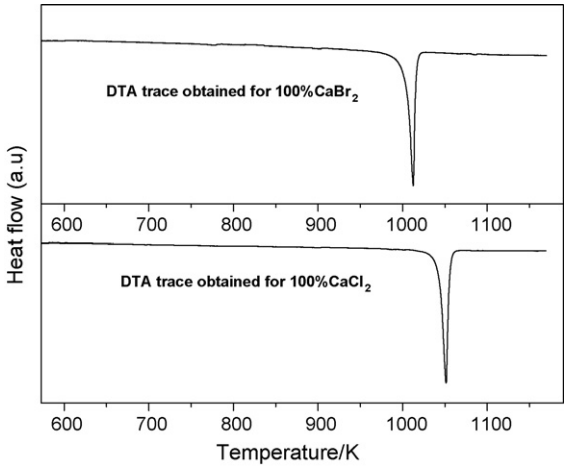

Fig. 1. DTA traces of pure $CaBr_2$ and $CaCl_2$.

neglected. Temperature calibration of the DTA unit was carried out using high purity metal standards: gold, silver, aluminium and zinc. For identifying the equilibrium phases that exist at high temperatures, samples of different compositions, namely 90, 75, 60, 45, 30 and 15 mol% taken in quartz tubes were melted followed by equilibration at 923 K under flowing hydrogen gas for 190 h. After the equilibration, the samples were quenched using liquid nitrogen and then the equilibrium phases were loaded in capillary tubes and characterized using XRD (Stoe Diffractometry, Bragg Brandano geometry). Similar experiments were carried out with samples equilibrated at 673 K for 400 h.

3. Results and discussion

The DTA traces obtained for pure components $CaBr_2$, $CaCl_2$ and for samples of nineteen compositions starting from 5 to 95 mol% $CaBr_2$ are shown in Figs. 1–3. Solidus temperatures and liquidus temperatures deduced from these DTA results for various compositions at a heating rate of 1 K/min are listed in Table 1. XRD results of the samples equilibrated at 923 and 673 K, followed by quenching in liquid N_2 and those of pure $CaBr_2$ and $CaCl_2$ are shown in Figs. 4 and 5, respectively.

Both the XRD patterns of the pure $CaBr_2$ and $CaCl_2$ could be assigned to orthorhombic structures [JCPDS file nos: 71-2044, 74-0522]. Examination of the DTA curve obtained for pure $CaCl_2$, shown in Fig. 1, indicates a single endothermic peak corresponding to its melting point at 1043 K which is in agreement with the value of 1046 K, reported in literature [9]. The observed melting point of $CaBr_2$ was 1011 K that was in close agreement to the values of 1015 and 1011 K reported in literature [10,11]. DTA traces of these pure phases indicate that there are no other phase transitions up to their melting points. DTA curves of all the other compositions also showed a single endothermic peak between room temperature and 1073 K. From the DTA curves of samples containing $CaBr_2$ and $CaCl_2$ shown in Figs. 2 and 3, the liquidus temperatures at which the DTA curves trace back to the base line were also recorded. It can be seen from the results shown in Table 1, which the liquidus temperatures decrease monotonically from the melting point of pure $CaCl_2$ up to ~55 mol% $CaBr_2$ and then increase monotonically further up to the melting point of pure $CaBr_2$. The results further indicate that the onset of endothermic peak for each composition also shows a similar trend, i.e., decrease in monotonically from the melting point of pure $CaCl_2$ up to ~55 mol% $CaBr_2$ and then increase monotonically further up to the melting point of pure $CaBr_2$. In a

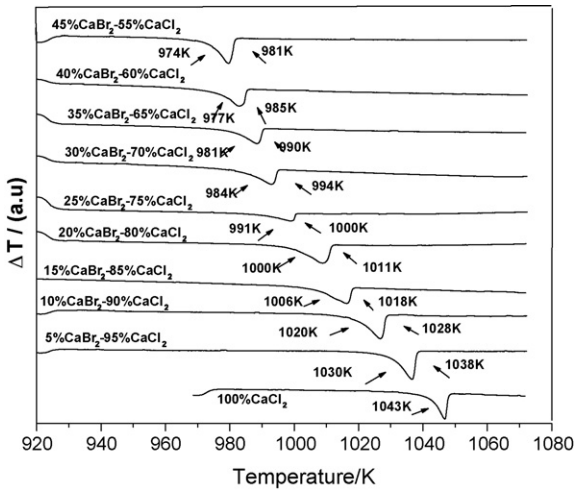

Fig. 2. DTA traces obtained for samples of $CaBr_2$–$CaCl_2$ system (Pure $CaCl_2$ to 55 mol% $CaCl_2$).

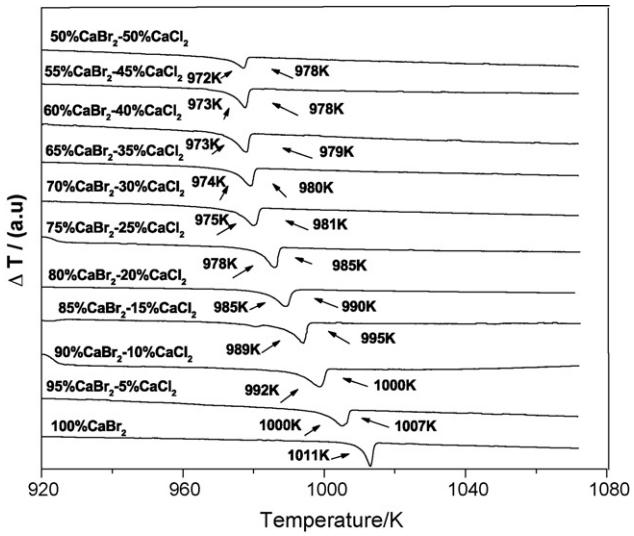

Fig. 3. DTA traces obtained for samples of $CaBr_2$–$CaCl_2$ system (Pure $CaBr_2$ to 50 mol% $CaBr_2$).

Table 1
DTA results for $CaCl_2$–$CaBr_2$ system.

S. no.	Composition of $CaCl_2$–$CaBr_2$ (mol%)	Onset temperature (K) (±1)	Liquidus temperature (K) (±1)
1	100–0	1043	–
2	95–05	1030	1038
3	90–10	1020	1028
4	85–15	1006	1018
5	80–20	1000	1011
6	75–25	991	1000
7	70–30	984	994
8	65–35	981	990
9	60–40	977	985
10	55–45	974	981
11	50–50	972	978
12	45–55	973	978
13	40–60	973	979
14	35–65	974	980
15	30–70	975	981
16	25–75	978	985
17	20–80	985	990
18	15–85	989	995
19	10–90	992	1000
20	05–95	1000	1007
21	0–100	1011	–

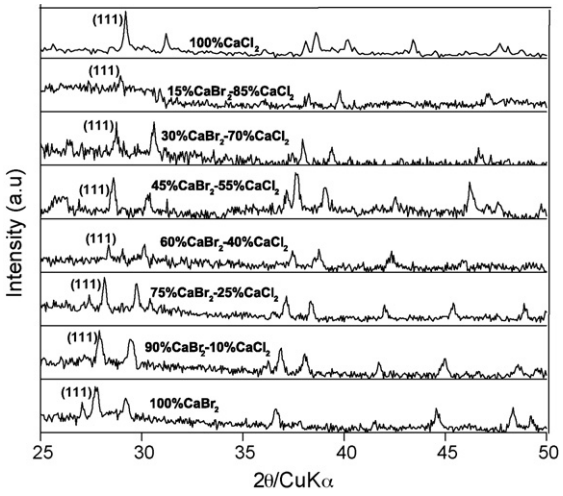

Fig. 4. XRD pattern of samples equilibrated at 923 K.

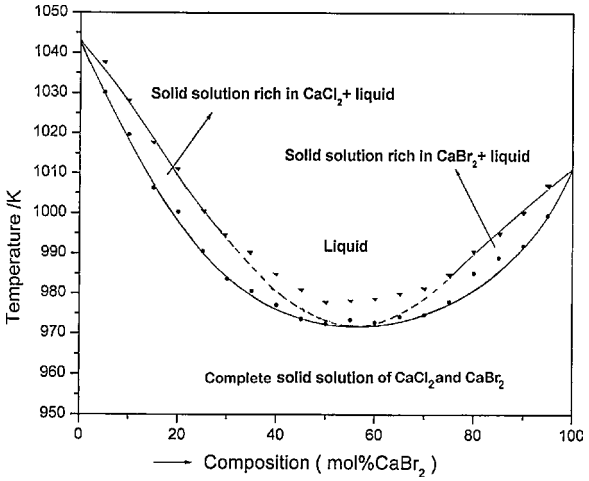

Fig. 6. Phase diagram of $CaCl_2$–$CaBr_2$ system.

binary system with no significant mutual solubility between the pure components, one expects a sharp endothermic peak for the eutectic reaction at eutectic temperature (an isothermal event) for a range of compositions. Further, this isothermal endothermic peak is expected to be followed by a broad tailing that retraces the base line at liquidus temperature for each composition. The absence of such a DTA pattern with isothermal peak indicates the $CaBr_2$–$CaCl_2$ system does not exhibit a simple eutectic reaction. On the other hand the observation of a monotonic variation of onset temperature of endothermic peaks with change in composition indicates that the components of the system exhibit mutual and complete solid solubility at high temperatures if not from room temperature onwards. The solid solution region is essentially a single-phase region and the degree of freedom in this region is two. This means that both temperature and composition can be changed in this region without appearance of another phase. On heating a solid solution of a known composition, liquid phase appears at a temperature which is characteristic of that composition and falls on the solidus curve as the degree of freedom is one. On further heating, more of liquid is formed due to preferential dissolution of either $CaCl_2$ or $CaBr_2$ solid into the liquid phase. The two-phase region would end ultimately at the liquidus temperature when the solid phase completely disappears. From all these observations made on DTA results, phase diagram of $CaBr_2$–$CaCl_2$ system is constructed and is shown in Fig. 6.

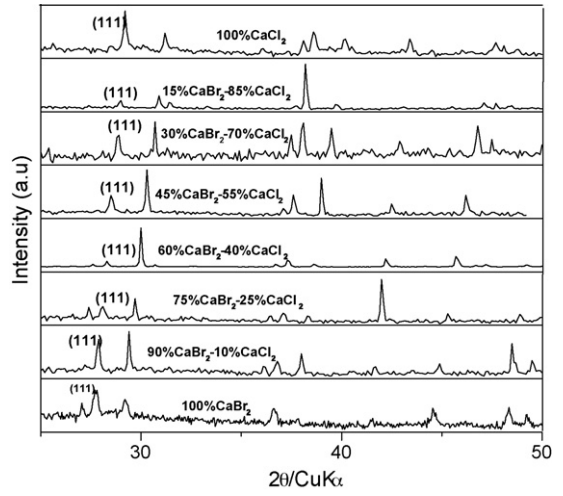

Fig. 5. XRD pattern of samples equilibrated at 673 K.

The phase diagram consists of the following four regions:
Complete solid solution of $CaCl_2$ and $CaBr_2$
Solid solution rich in $CaCl_2$ + liquid
Solid solution rich in $CaBr_2$ + liquid
Liquid

The minimum in the liquidus curve shown in Fig. 6 is at 56.5 mol% $CaBr_2$ and at 971 K where it would meet the solidus curve. It is noted here that the DTA curves of samples of this system showed a width of 6 and 4 K even for the endothermic peaks of the melting of pure $CaCl_2$ and $CaBr_2$, respectively. Hence at compositions near the minimum of liquidus temperatures, the experimentally measured liquidus points are found to be outside the liquidus curve shown as dotted line. Further, on decreasing sample size to ~4 mg the width did not come down both for the pure compounds and compositions. The fact that the liquidus curve shows a minimum at 56.5 mol% $CaBr_2$ instead of a continuous monotonic increase from pure $CaBr_2$ to pure $CaCl_2$, indicates that this system may exhibit a region where two limited solid solutions co-exist, probably at lower temperatures. Evidence of this possibility could not be obtained from the DTA results as DTA curves of all the compositions showed a single endothermic peak between 298 and 1073 K. Also, XRD results obtained for 100% $CaBr_2$, 100% $CaCl_2$ and for the phases obtained after long-term equilibration of compositions 90, 75, 60, 45, 30 and 15 mol% $CaBr_2$ at 923 and 673 K, qualitatively agreed with the DTA results. The samples are moisture sensitive in nature and the equilibrated phases were taken in Lindemann capillary tubes and sealed gas tight with wax inside argon glove box. Due to the small sample size, the XRD pattern obtained could be used only to characterize the phases as the signal to noise ratio of many XRD peaks are moderate. It could be seen from Figs. 4 and 5 that the XRD pattern is nearly the same for different compositions and only shifting of major XRD peaks are observed with compositional change. From the X-ray data of the most intense peak obtained for 1 1 1 plane, which showed high signal to noise ratio, we calculated the d_{111} values and are given in Table 2. These values are plotted against composition of $CaBr_2$ in Fig. 7 and the fitted curve is found to vary linearly from pure $CaCl_2$ to pure $CaBr_2$. The fact that both phases $CaCl_2$ and $CaBr_2$ belong to the same crystal structure namely, orthorhombic and the ionic radii of Cl^- and Br^- are very close (1.81 and 1.96 Å, respectively [12]), satisfy the condition needed for complete solid solution formation of these two phases. Fig. 7 indicates that when the bulkier bromide ions substitute for the smaller chloride ions with increasing composition of $CaBr_2$, the lattice probably experiences isotropic expansion. More detailed analysis of X-ray data is not possible with these X-ray data and

Table 2
Variation of lattice constant, $d_{111,}$ with composition of samples equilibrated at 923 and 673 K.

Compositions (mol%$CaBr_2$)	d_{111} (Å) (equilibrated at 923 K)	d_{111} (Å) (equilibrated at 673 K)
100	3.2009	3.2009
90	3.1956	3.1951
75	3.1680	3.1730
60	3.1460	3.1510
45	3.1186	3.1294
30	3.1029	3.0974
15	3.0818	3.0765
0	3.0559	3.0559

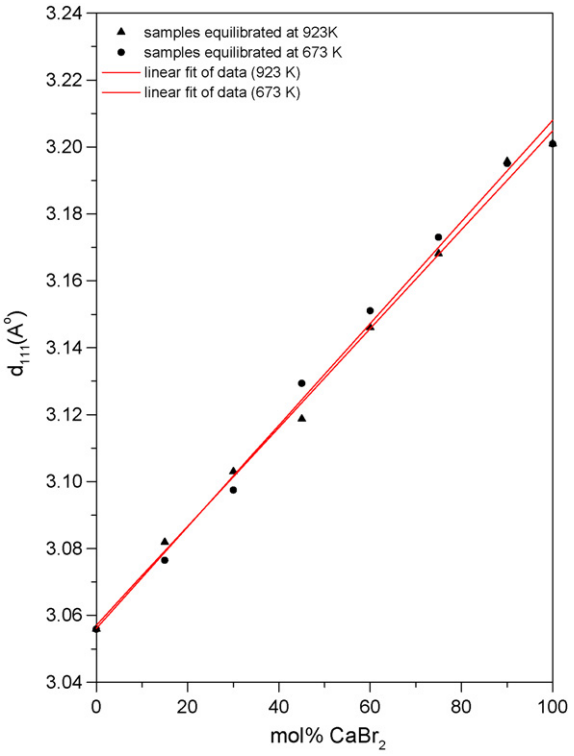

Fig. 7. Linear variation of lattice constant with composition of $CaBr_2$.

the linear increase of d_{111} values observed for equilibrated samples with increase in composition of $CaBr_2$, qualitatively support the formation of complete solid solution. All these results corroborate the fact that there are no terminal solid solution regions and gives discernible evidence for complete solid solution between 923 K > T > 673 K.

4. Conclusion

The phase diagram of $CaCl_2$–$CaBr_2$ system is constructed based on DTA analysis of samples with compositions in the range of 100% $CaCl_2$ to 100% $CaBr_2$ in steps of 5 mol% and the XRD results of samples of several compositions equilibrated at 923 and 673 K. The solidus and liquidus curve exhibit a minimum at 971 K and at a composition of 56.5 mol% $CaBr_2$.

Acknowledgements

The authors gratefully acknowledge Dr. H.N. Jena and Dr S. Kalavathi for their help in characterization of materials by XRD and Shri R. Aswathraman for his help in data treatment of XRD patterns.

References

[1] C.A. Smith, Berkeley Nuclear Laboratories, Central Electricity Generating Board, U.K., Report R/D/BN-2331 (1972).
[2] R.B. Holden, N. Fuhrman, Proceedings of the International Conference on Sodium Technology and Large Fast Reactor Design. Atomic Energy Commission Report, ANL-7520-1, Argonne, Illinois, U.S., 7–9 November 1968, 1968, p. 262.
[3] T. Gnanasekaran, K.H. Mahendran, R. Sridharan, V. Ganesan, G. Periaswami, C.K. Mathews, Nucl. Technol. 90 (1990) 408–416.
[4] R. Sridharan, K.H. Mahendran, T. Gnanasekaran, G. Periaswami, U.V. Varada Raju, C.K. Mathews, J. Nucl. Mater. 223 (1995) 72–79.
[5] R. Sridharan, K.H. Mahendran, S. Nagaraj, T. Gnanasekaran, G. Periaswami, J. Nucl. Mater. 312 (2003) 10–15.
[6] Kitheri Joseph, K. Sujatha, S. Nagaraj, K.H. Mahendran, R. Sridharan, G. Periaswami, T. Gnanasekaran, J. Nucl. Mater. 344 (2005) 285–290.
[7] K.H. Mahendran, S. Nagaraj, R. Sridharan, T. Gnanasekaran, J. Alloys Compd. 325 (2001) 78–83.
[8] K.H. Mahendran, K. Sujatha, R. Sridharan, T. Gnanasekaran, J. Alloys Compd. 358 (2003) 42–47.
[9] M. Yamada, M. Tago, S. Fukusako, A. Horibe, Thermochim. Acta 218 (1993) 401–411.
[10] M.W. Chase Jr., C.A. Davies, J.R. Downey Jr., D.R. Frurip, R.A. McDonald, A.N. Syverud (Eds.), JANAF thermochemical tables, third ed. Part 1, Al–Co, J. Phys. Chem. Ref. Data 14 (Suppl. 1) (1985) 461–464.
[11] B.A.O. Xinhua, C.H.E.N. Nianyi, L.U. Wencong, CHENG. Zhihuan, L.U.O. Yunyun, L.U. Weiying, X.I.A. Yiben, Rare Met. 25 (2006) 293–296.
[12] R.D. Shannon, Acta Crystallogr. A32 (1976) 751–767.